

# Electrochemical and Quantum Chemical Assessment of Some Thiosemicarbazide Derivatives as Carbon Steel Corrosion Inhibitors in HCl; Continuously Monitoring the Current Change by FFT Voltammetry

Shirin Shahabi<sup>1</sup>, Parviz Norouzi<sup>1,2,\*</sup>

<sup>1</sup> Center of Excellence in Electrochemistry, School of Chemistry, University of Tehran, Tehran, Iran

<sup>2</sup> Biosensor Research Center, Endocrinology & Metabolism Molecular-Cellular Sciences Institute, Tehran University of Medical Sciences, Tehran, Iran

\*E-mail: [norouzi@khayam.ut.ac.ir](mailto:norouzi@khayam.ut.ac.ir)

Received: 18 December 2016 / Accepted: 11 February 2017 / Published: 12 March 2017

---

In this study, Firstly, two synthesized thiosemicarbazide derivatives, N-(2-(2-methoxyphenyl)hydrazinecarbonothioyl)benzamide (TSC4) and N-(2-(furan-2-carbonyl)hydrazinecarbonothioyl)benzamide (TSC5), were investigated as carbon steel corrosion inhibitors in 1.0 M HCl by potentiodynamic polarization (PDP), electrochemical impedance spectroscopy (EIS), fast Fourier transform continuous cyclic voltammetry (FFTCCV) and scanning electron microscopy (SEM). PDP results showed the mixed-type inhibition with predominantly anodic effect. EIS experiments showed the increase in polarization resistance and decrease in double layer capacitance by inhibitors adsorption. The maximum IE% values for the solutions containing  $1.0 \times 10^{-3}$  M TSC4 and TSC5 were equal to 94.0% and 94.9%, respectively. FFTCCV results indicated that in addition to inhibition efficiencies, the rate of adsorption for TSC5 is higher than TSC4. In the next step, quantum chemical studies were performed for a five member group of thiosemicarbazide derivatives and revealed that among the calculated electronic parameters,  $\Delta E$ , the energy gap between HOMO and LUMO, exhibited the maximum correlation ( $R^2=0.97$ ) with %IE. SEM analysis showed improvements of the surface characteristics in the presence of studied inhibitors.

---

**Keywords:** Corrosion inhibition; Carbon steel; Quantum chemical calculations, FFT Voltammetry

## 1. INTRODUCTION

Corrosion of metallic materials has been an inevitable part of the human experience. So, because of the safety, economics and conservation problems resulting from corrosion effects, we need to study about corrosion and find ways to its control. Carbon steel is an alloy that consists of iron and

carbon. Despite its relatively limited corrosion resistance, carbon steel is frequently used in various applications such as nuclear and fossil fuel power plants, transportation, chemical processing, mining, construction, and metal processing equipment. All of these areas undergo corrosion problems in some extent [1]. Acids are widely used in many branches of industry. Examples are synthesis processes in the chemical and petrochemical industry, chemical cleaning before galvanizing, phosphatizing, passivation, or other coating uses [2]. Acid pickling of steel is necessary to remove mill scale from the surface.

Iron or carbon steel in contact with acids and other electrolytes will corrode with the electrochemical mechanism. Corrosion in acid solutions can be reduced by addition of chemical compounds, which named as corrosion inhibitors. In pickling baths, the inhibitors protect metal surface from corrosive action of acids while the pickling performance of the system maintains [3]. Varieties of organic compounds have been used as inhibitors [4-10]. These compounds are chemically or/and physically adsorbed on the metal surface, which form a monolayer that hinders both the anodic and cathodic reactions.

Recently, thiosemicarbazide compounds (having  $\text{NH}_2\text{CSNHNH}_2$  as functional group) have attracted much consideration because of their antiviral, antitumor, and antimicrobial properties [11-18], as well as other industrially important activities, including anticorrosion and antifouling effects [19-25]. Considering their good inhibitive properties and ease of synthesis, it is attractive to synthesize new series of thiosemicarbazides with the purpose of using as corrosion inhibitors.

Density functional theory (DFT) is a quantum mechanical modelling method in physics and chemistry to explore the electronic structure of atoms, molecules and condensed phases. Using this theory, the properties of many-electron systems can be determined with functions. Over the past 25 years, DFT has become a valuable tool in most fields of chemistry. Many experimental investigations in organic and inorganic chemistry use DFT calculations for giving further information. It finds applications in determining various properties, which can be found using various experimental methods [26]. In the last decade, there is an increasing interest in the utilization of quantum chemical calculation methods in the area of corrosion science [27-34]. These methods give molecular properties that might be useful in selecting corrosion inhibitors among a list of potential molecules as possible candidates for corrosion inhibition. In addition, quantum chemical calculation methods are very useful in explaining the experimental results and inhibition mechanism.

In this paper, firstly we synthesized two substituted thiosemicarbazide compounds, N-(2-(2-methoxyphenyl)hydrazinecarbonothioyl)benzamide (TSC4) and N-(2-(furan-2-carbonyl)hydrazinecarbonothioyl)benzamide (TSC5), and investigated their effect on carbon steel corrosion in 1.0 M HCl, by potentiodynamic polarization (PDP), electrochemical impedance spectroscopy (EIS), fast Fourier transform continuous cyclic voltammetry (FFTCCV) and scanning electron microscopy (SEM). Then, quantum chemical calculations were performed to calculate some electronic parameters of the studied compounds. The calculation results were merged with the results for three compounds with similar structures, which have been previously investigated as carbon steel corrosion inhibitors by our research team [35,36]. In order to understand the relationship between the structural and electronic characteristics of five thiosemicarbazide derivatives and their inhibition efficiencies (IE%), the values of calculated parameters were correlated with the IE% values.

## 2. MATERIALS AND METHODS

### 2.1. Inhibitors structures and solutions

Figure 1 shows the chemical structures of the thiosemicarbazide compounds, which their inhibitive effect on carbon steel corrosion were investigated in this paper. Among them, N-(2-(2-methoxyphenyl)hydrazine carbonothioyl)benzamide (TSC4) and N-(2-(furan-2-carbonyl)hydrazinecarbonothioyl)benzamide (TSC5) were newly synthesized and experimentally investigated in the present study. On the other hand, 2-Carbamothioyl-N-phenylhydrazinecarboxamide (TSC1), N1-phenyl-1,2-hydrazinedicarbothioamide (TSC2) and N-[(2-Carbamothioylhydrazino)carbonothioyl] benzamide (TSC3) were investigated in our previous works [35,36] as carbon steel corrosion inhibitors. In this work, the previously obtained results were merged with new results to get more comprehensive explanations for the inhibitory effect of these compounds.

To synthesize TSC4 and TSC5, a mixture of ammoniumthiocyanate and HCl was warmed at about 50°C for 5 min. Then, a definite amount of 2-methoxyphenylhydrazine and furan 2-carbohydrazide was respectively added to obtain TSC4 and TSC5. The mixture was stirred for 3 h at room temperature, and at the end, poured into 15 mL of water. The obtained precipitation was separated by filtration and recrystallized from ethanol to obtain the pure compounds.

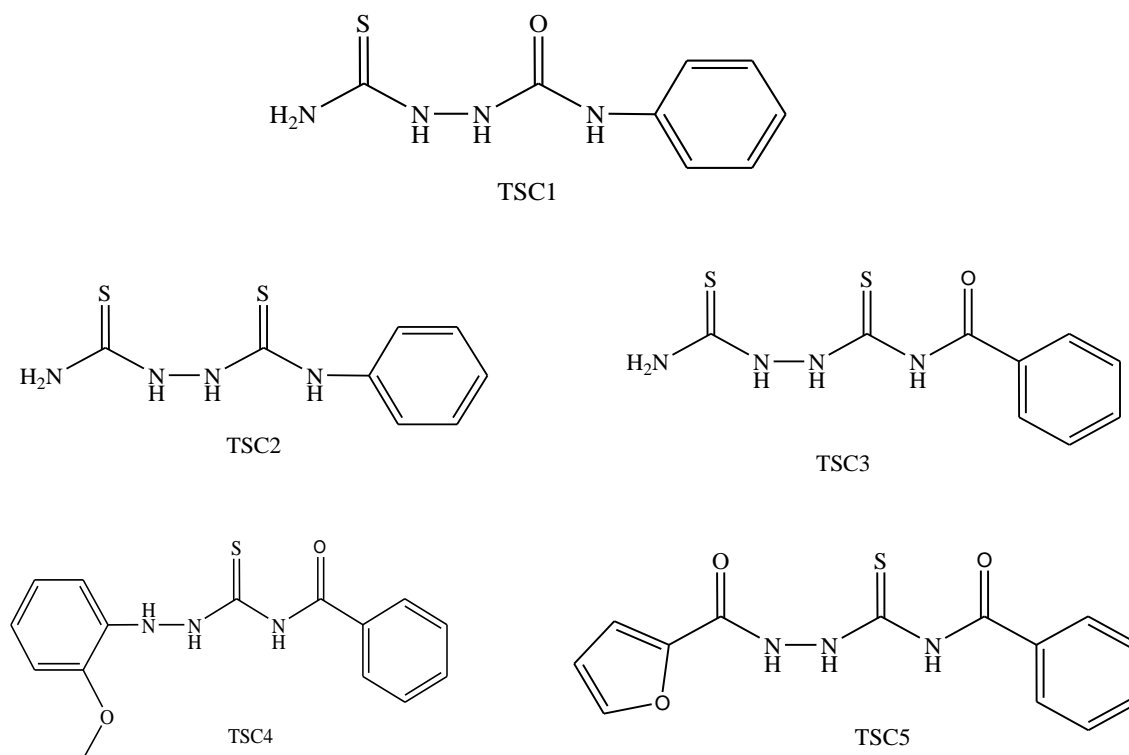


**Figure 1.** Molecular structures of the inhibitors TSC1, TSC2, TSC3, TSC4 and TSC5.

Because of the solubility problems, the inhibitor solutions were prepared in 1.0 M HCl containing 5 % v/v DMSO. Obviously, this volume of DMSO was also added to the blank solution.

The corrosive solution of 1.0 M HCl was prepared by dilution of 36 % HCl (from Merck) with distilled water.

## 2.2. Electrochemical measurements

All electrochemical studies were performed with a three-electrode set-up containing a carbon steel working electrode (WE), a Pt counter electrode (CE) and an Ag/AgCl reference electrode (RE). The carbon steel samples contained C 0.326 %, Si 0.235 %, Mn 0.742 %, P 0.016 %, Cr 0.073 %, Ni 0.015 %, Al 0.022 %, S 0.017 %, Cu 0.129 %, V 0.002 % and the rest iron. The working electrode was constructed from a cylindrical carbon steel bar mounted in epoxy resin to give an exposed surface of 5 mm diameter. At the first of each measurement, the electrode surface was polished with different grades of emery papers (which ended with the 1200 grit), degreased in ultrasonic bath with ethanol and acetone and finally rinsed with distilled water.

PDP and EIS experiments were performed using an AUTOLAB model PGSTAT30 containing a frequency response analyzer. Prior to each experiment, the fresh surface of WE was immersed in the test solution for 45 minutes to reach a steady state open circuit potential ( $E_{ocp}$ ).

To obtain polarization curves, the potential was swept from a more positive potential than  $E_{ocp}$  to a more negative potential than  $E_{ocp}$  at a scan rate of 1.0 mV/s. The curves were recorded using a personal computer, which was connected to the electrochemical instrument. The polarization data was analyzed using GPES electrochemical software.

EIS experiments were carried out at  $E_{ocp}$  by superimposing a sinusoidal potential of 5.0 mV amplitude at frequencies between  $1.0 \times 10^5$ - $5.0 \times 10^{-2}$  Hz. EIS data were analyzed with FRA software.

At each FFTCCV run, cyclic voltammograms were obtained repeatedly by sweeping the potential between an initial and a final potential that includes corrosion potential ( $E_{corr}$ ). To perform FFTCCV experiments, a set-up containing a PC equipped with a data acquisition board (PCL-818HG, Advantech. Co.) and a custom-made potentiostat was used. Due to the instrument limitations, the CV measurements were carried out at 1.0 V/s, which was the lowest possible scan rate that could be used to collect the data. Using the ability of displaying the cyclic voltammograms as three-dimensional graphs and the calculation of the total charge under the curves, the changes in current and charge passed through the electrode have been continuously monitored.

## 2.3. SEM measurements

The surface morphology of carbon steel samples was observed using a scanning electron microscope (Hitachi 460). The carbon steel surface was prepared by keeping the specimens for 24 h in 1.0 M HCl with and without inhibitors, after abraded using different emery papers up to 1200 grit size. After this immersion time, the specimens were washed gently with distilled water, carefully dried and inserted into the scanning electron microscope.

#### 2.4. Quantum chemical calculations

The geometrically optimization of molecular structures of the studied inhibitors were done by Gaussian03 [37] software using the density functional theory (DFT) at the B3LYP/6-31G(d,p) level, based on the absence of imaginary frequencies. The calculated quantum chemical parameters are the highest occupied molecular orbital energy ( $E_{\text{HOMO}}$ ), the lowest unoccupied molecular orbital energy ( $E_{\text{LUMO}}$ ), the energy gap between HOMO and LUMO ( $\Delta E$ ) and the dipole moment (D).

### 3. RESULTS AND DISCUSSION

#### 3.1 PDP measurements

The Tafel plots obtained by polarization measurements of the carbon steel electrode in the absence and presence of various concentrations of TSC4 and TSC5 are respectively shown in Figure 2a and b. As shown in the figure, the Tafel plot of the carbon steel electrode slightly shifts to more positive potentials after the addition of TSC4 and TSC5. Using Tafel extrapolation method, the electrochemical polarization parameters of the carbon steel corrosion reaction was extracted from the Tafel plots and listed in Table 1. These parameters include the corrosion potential ( $E_{\text{corr}}$ ), the corrosion current density ( $I_{\text{corr}}$ ), the anodic ( $b_a$ ) and cathodic ( $b_c$ ) Tafel slope, and the inhibition efficiency (IE%). The values of IE% were calculated according to Eq. (1) [38]:

$$\text{IE\%} = \frac{I_{\text{corr, uninhibit}} - I_{\text{corr, inhibit}}}{I_{\text{corr, uninhibit}}} \times 100 \quad (1)$$

where the  $I_{\text{corr, uninhibit}}$  and  $I_{\text{corr, inhibit}}$  are the corrosion current density without and with inhibitors, respectively. The plots shown in Figure 2 and the  $I_{\text{corr}}$  values in Table 1 illustrate that with addition of the inhibitors, the value of  $I_{\text{corr}}$  decreases from  $461.3 \mu\text{A cm}^{-2}$  to lower values, which are related to the inhibitors concentration. With increasing the inhibitors concentration, the  $I_{\text{corr}}$  values decrease and the quantities of IE% increase. The maximum of inhibition efficiency was obtained 94.4% for  $1.0 \times 10^{-3}$  M TSC5. The maximum value of IE% in the presence of TSC4 is equal to 93.8% for the solution  $1.0 \times 10^{-3}$  M. These results demonstrate that TSC5 can better inhibit the carbon steel corrosion in HCl solution. The data in Table 1 also show that by addition of the inhibitors, both anodic and cathodic Tafel slopes change in some extent. This observation proves that the inhibitors adsorb on the carbon steel surface and block the active sites of the corrosion reaction. This blocking retards either anodic dissolution of Fe atoms or cathodic reduction of  $\text{H}^+$  ions. The values of  $b_a$  and  $b_c$  are slightly increased demonstrating the slower kinetic of both half-reactions in the presence of inhibitors, but the mechanism of the corrosion reaction doesn't change.

As mentioned above, after the inhibitors addition, the Tafel plot of carbon steel electrode displaces toward more positive potentials. The maximum shift in  $E_{\text{corr}}$  was observed for the solution containing  $1.0 \times 10^{-3}$  M TSC5, which equals 40 mV toward anodic potentials.

These observations are associated with characteristics of mixed-type or adsorptive inhibitors. So, from polarization results, it could be concluded that TSC4 and TSC5 are mixed-type corrosion inhibitors with predominantly anodic inhibition effect [39-42].

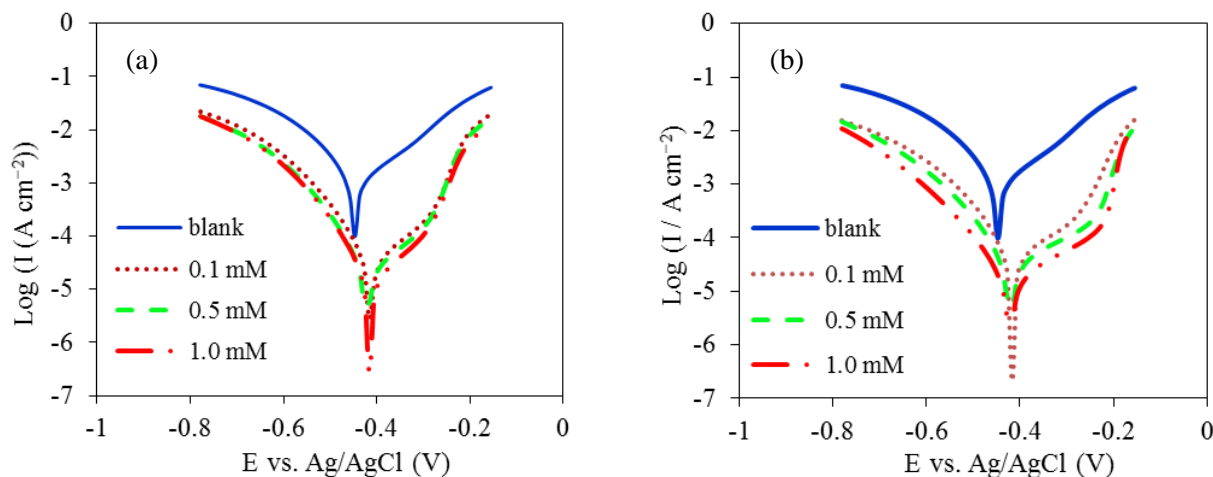


**Figure 2.** Polarization curves of carbon steel electrode in 1.0 M HCl without and with different concentrations of TSC4 (a) and TSC5 (b).

**Table 1.** Polarization parameters for carbon steel electrode in 1.0 M HCl solution in the absence and presence of various concentrations of the inhibitors TSC4 and TSC5.

Inhibitor	C <sub>inh</sub> (M)	-E <sub>corr</sub> (mV)	I <sub>corr</sub> (μA cm <sup>-2</sup> )	-b <sub>c</sub> (mV dec <sup>-1</sup> )	b <sub>a</sub> (mV dec <sup>-1</sup> )	IE (%)
Blank	-	455	461.3	137	111	-
TSC4	1.0×10 <sup>-4</sup>	422	39.2	139	118	91.5
	5.0×10 <sup>-4</sup>	425	37.4	138	118	91.9
	1.0×10 <sup>-3</sup>	423	28.61	143	119	93.8
TSC5	1.0×10 <sup>-4</sup>	414	38.7	142	118	91.6
	5.0×10 <sup>-4</sup>	414	33.2	142	125	92.8
	1.0×10 <sup>-3</sup>	415	25.8	144	131	94.4

### 3.2. EIS results

EIS has been successfully applied to the study of corrosion systems for thirty years. EIS data for the corrosion processes are most often represented in Nyquist plots as shown in Figure 3a and b, in which the diagrams show the EIS data for the carbon steel electrode in the absence and presence of various concentrations of TSC4 and TSC5. As can be seen in Figure 3 a and b, the Nyquist plots have the shape of one depressed semicircle, the diameter of which is increased with the inhibitors concentration. Such semicircle shape in the impedance data indicates that the reaction is activation-

controlled with one charge-transfer reaction. The presence of a single capacitive loop is an indication of one time-constant of the electrical double layer at the metal/solution interface. In order to access the charge transfer resistance or polarization resistance that is proportional to the corrosion rate at the interface, EIS results were interpreted with the help of a circuit model of the interface, which is shown in Figure 4. In the circuit, CPE is the constant phase element,  $R_s$  is the solution resistance and  $R_p$  is the polarization resistance.  $R_s$  is equal to the resistance at high frequencies and  $R_p$  equals the semicircles diameters. This circuit is commonly used for the description of such Nyquist plots of the metal/solution interface in corrosion systems [43-47]. The model is based on the simple Randles circuit [48], in which the double layer capacitor is replaced by a constant phase element (CPE). The CPE is used to account for the non-ideal behavior of the double layer at the interface, which caused some depression in the Nyquist semicircles. This non-ideality comes from the inhomogeneities existing in the solid electrode surfaces. The impedance function of a CPE is equated as below [49]:

$$Z_{\text{CPE}} = Q^{-1} (j\omega)^{-n} \quad (2)$$

where  $Q$  is the magnitude of CPE,  $j$  is the imaginary number,  $\omega$  is the sine wave angular frequency ( $\omega = 2\pi f$ , the frequency in Hz) and  $n$  is the CPE exponent (phase shift), which could be used to explain the degree of surface inhomogeneity and non-ideality in capacitor behavior. For  $n=0$ , 1 and  $-1$ , the CPE denotes a pure resistor, capacitor and inductor, respectively. The impedance parameters of the studied corrosion system including  $R_p$ ,  $Q$ ,  $n$  and IE% are shown in Table 2. The values of IE% in Table 2 were calculated by the following equation:

$$\text{IE \%} = \frac{R_{p,\text{inhibit}} - R_{p,\text{uninhibit}}}{R_{p,\text{inhibit}}} \times 100 \quad (3)$$

where  $R_{p,\text{inhibit}}$  and  $R_{p,\text{uninhibit}}$  are the polarization resistance of inhibited and uninhibited solutions, respectively.

The data in Table 2 represent that with addition of the inhibitors,  $R_p$  values increased and conversely,  $Q$  values decreased. The reduction of  $Q$  values is evidence for the substitution of the water molecules and the ions, which initially adsorbed on the carbon steel surface, with inhibitors larger molecules with lower dielectric constants. This substitution causes the extension of the double layer thickness and as a result, the reduction in its capacitance. The adsorption of inhibitor molecules on the carbon steel surface forms a barrier between the steel surface and the corroding medium. This protects the Fe atoms below the organic layer from the corrosive attack. This adsorption leads to an increase in the  $R_p$  value of the corrosion reaction as it is shown by the data in Table 2. The highest  $R_p$  value ( $1124.5 \Omega \text{ cm}^2$ ) was obtained by TSC5 at  $1 \times 10^{-3} \text{ M}$  concentration, leading to the maximum IE% value (94.9%). The lowest  $R_p$  value ( $672.2 \Omega \text{ cm}^2$ ) and consequently the minimum inhibition efficiency (91.4%) was obtained by TSC4 at  $1 \times 10^{-4} \text{ M}$  concentration. The higher value of  $R_p$  is generally associated with the slower corrosion reaction and accordingly, the higher inhibition efficiency [50-52].

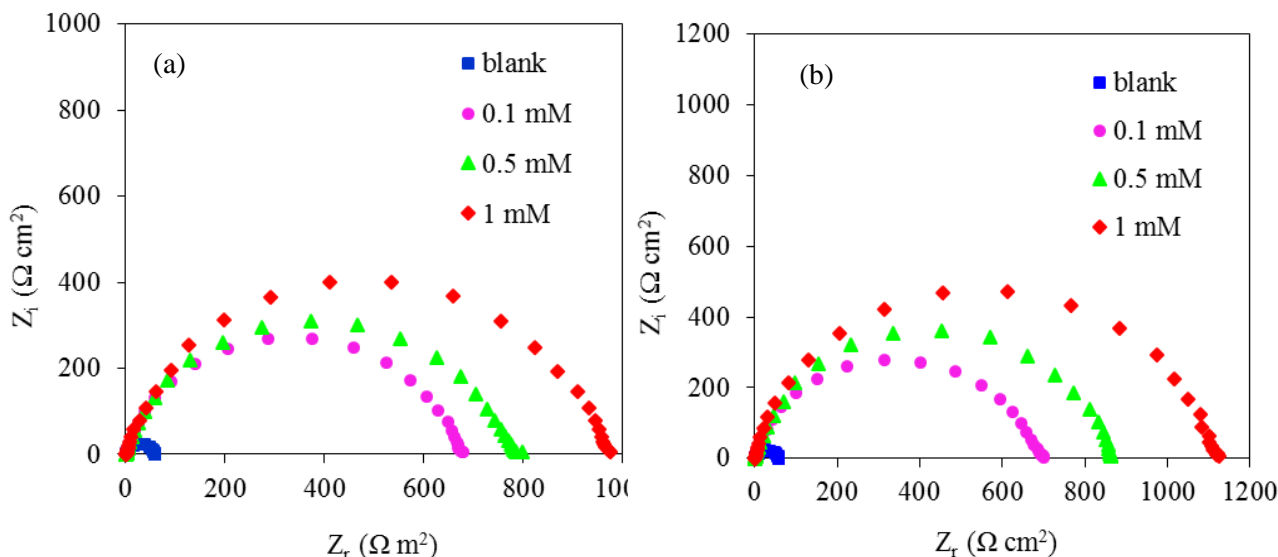


**Figure 3.** Nyquist Impedance plots of carbon steel electrode obtained in 1.0 M HCl in the presence of various concentrations of TSC4 (a) and TSC5 (b).

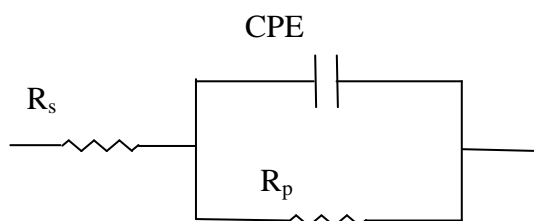


**Figure 4.** Electrical equivalent circuit used to fit the impedance data.

The values of  $n$  are in the range between 0.85 and 0.9. Generally, with increasing the  $R_p$  values, the values of  $n$  are also increased, showing the smoother electrode surface. A comparison between the data in Tables 1 and 2 shows that the results of the PDP and the EIS methods are comparable and run parallel with each other.

**Table 2.** Electrochemical impedance parameters for carbon steel electrode in 1.0 M HCl in the absence and presence of various concentrations of the inhibitors TSC4 and TSC5.

Inhibitor	$C_{inh}$ (M)	$R_p$ ( $\Omega\text{ cm}^2$ )	$n$	$Q$ ( $\mu\Omega^{-1}\text{ s}^n\text{ cm}^{-2}$ )	IE (%)
Blank	–	57.8	0.86	305.7	–
TSC4	$1.0 \times 10^{-4}$	672.2	0.87	27.3	91.4
	$5.0 \times 10^{-4}$	781.2	0.86	21.5	92.6
	$1.0 \times 10^{-3}$	965.9	0.88	17.9	94.0
TSC5	$1.0 \times 10^{-4}$	692.1	0.87	24.3	91.6
	$5.0 \times 10^{-4}$	862.9	0.89	20.7	93.3
	$1.0 \times 10^{-3}$	1124.5	0.90	14.4	94.9

3.3. FFTCCV experiments

By applying FFTCCV, it could be possible to follow the current and the charge passed through the carbon steel electrode, continuously. So, the changes of them could be related to the changes of the electrode surface during the experiments. In FFTCCV, during each experiment, the potential waveform (Figure 5) was continuously applied to the electrode. As a result, we have numerous cyclic voltammograms.

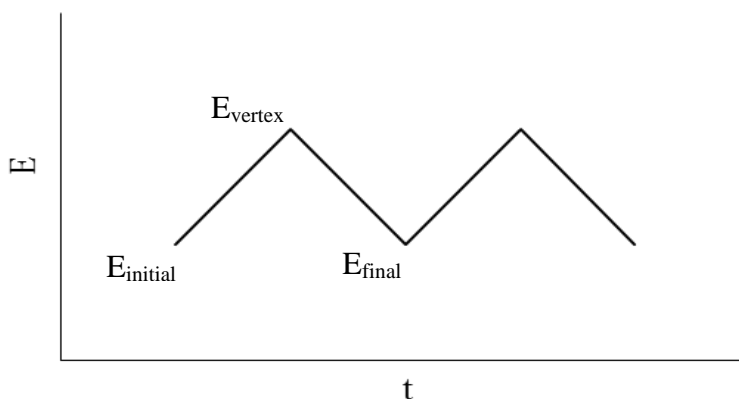
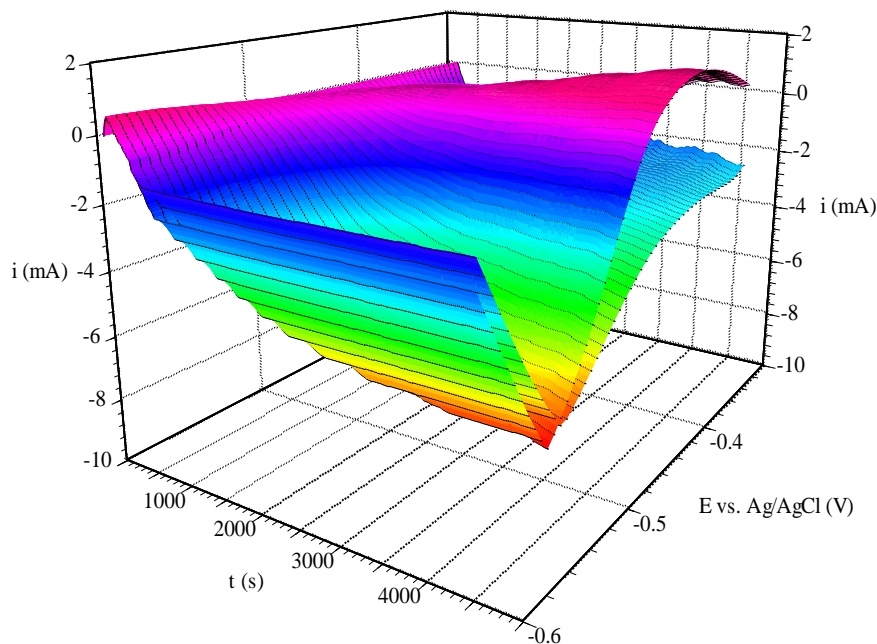
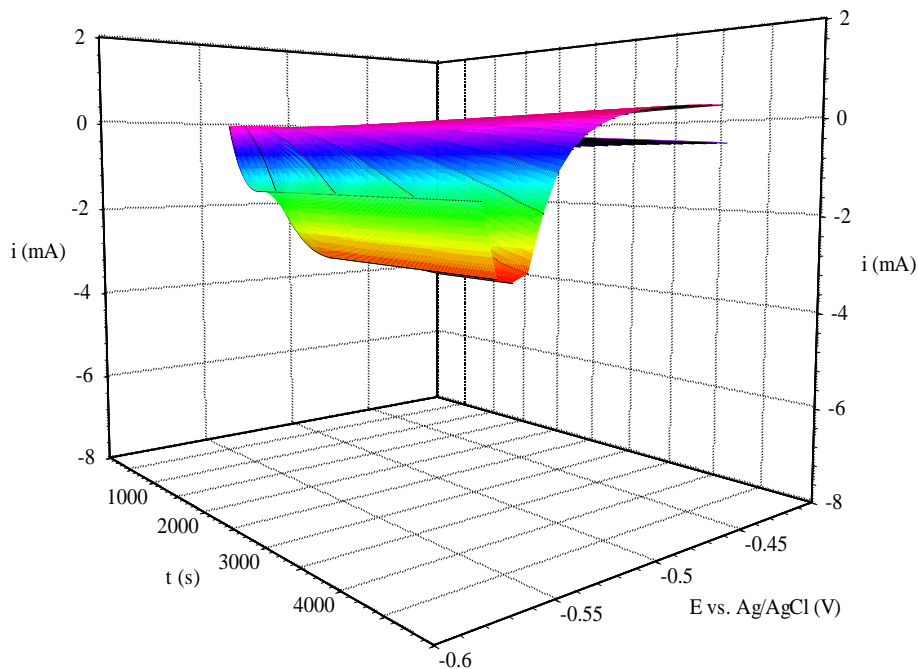


Figure 5. Diagram of the applied potential waveform in FFTCCV experiments.

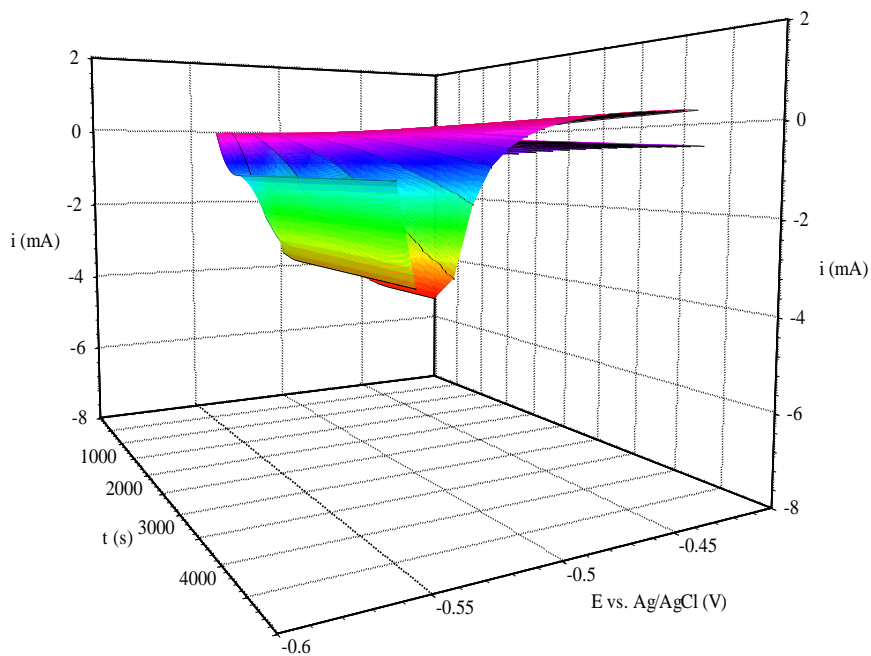
The background current in voltammetric measurements could be removed from the recorded voltammograms. This provides information about the adsorption processes and changes in the double layer at the electrode surface.



(a)



(b)



(c)

**Figure 6.** Recorded differential cyclic voltammograms of carbon steel electrode during 70 minutes immersion 1.0 M HCl without inhibitors (a) and with  $5.0 \times 10^{-4}$  M TSC4 (b) and TSC5 (c).

The following equation was used for background subtraction in the software program [53-56]:

$$\Delta I(s, E) = I(s, E) - I(s_r, E) \tag{4}$$

where  $s$  is the sweep number,  $I(s, E)$  represents the CV curve recorded during the  $s$ -th sweep and  $I(s_r, E)$  is the reference CV curve. The reference CV curve was obtained by averaging three CV

curves recorded at the beginning of each experiment. In practice, CV curves are recorded numerically by sampling current in equal time intervals. Figure 6a, b and c respectively show the typical continuous CV curves of the carbon steel electrode after 70 minutes immersion in 1.0 M HCl in the absence and presence of TSC4 and TSC5 at  $5.0 \times 10^{-4}$  M concentration. It can be seen in the figure that the net current change in the solution without inhibitors (up to 8.0 mA) is obviously larger than the current change in the presence of TSC4 (up to 3.4 mA) and TSC5 (up to 3.2 mA). This is an indication of the carbon steel corrosion inhibition by two studied thiosemicarbazide derivatives. In addition, it could be concluded that TSC5 can better retard the corrosion reaction than TSC4. These results confirm the PDP and EIS conclusions. The three-dimensional continuous CV curves in Figure 6a, b and c also demonstrate that for the solution containing TSC4 and TSC5, the maximum of the curves reaches to nearly constant value after 1500 s and 1300 s, respectively. It can be said that the adsorption of TSC5 takes place faster than TSC4. So, the inhibitor TSC5 reaches to its maximum surface coverage at shorter time.

For more investigation of the inhibitors adsorption behavior, the current was integrated at specific potential range to calculate the charge passed through the electrode.

The charge under cyclic voltammogram at the potential range  $E_1$  to  $E_2$ , which contains the corrosion potential, was calculated according to Equation 5.

$$Q_t = \frac{1}{v} \int_{E_1}^{E_2} I(E) dE \quad (5)$$

where  $v = dE/dt$  is the scan rate. In addition, the following equation is used with the computer program to integrate the current over the potential range,  $E_1$  to  $E_2$ , and calculate the overall charge ( $\Delta Q$ ) passed through the electrode at the specific potential window, [53, 57-59]:

$$\Delta Q(s,t) = \Delta t \left( \sum_{E=E_1}^{E=E_2} I(s,E) - \sum_{E=E_1}^{E=E_2} I(s_r,E) \right) \quad (6)$$

where  $s$  is the sweep number,  $t$  is the time period between subsequent sweeps,  $\Delta t$  is the time difference between two subsequent points on the CV curves,  $I(s, E)$  represents the CV curve recorded during the  $s$ -th sweep and  $I(s_r, E)$  is the reference CV curve. Figure 7 shows the calculated  $\Delta Q$  for the carbon steel electrode during 70 minutes immersion in 1.0 M HCl in the absence and presence of the compounds TSC4 and TSC5. From the slope of  $\Delta Q$  change vs. time, it can be deduced that presence of TSC4 and TSC5 leads to lessening the corrosion reaction rate. Like that previously seen in the Figure 6 for CV curves, the  $\Delta Q$ - $t$  plots at the inhibitor containing solutions also reach to nearly unchanged values at the end of each experiment and the electrode in the solution containing TSC5 reaches to this plateau at the shorter time than TSC1. These findings confirm that besides TSC5 reaches the maximum surface coverage in the shortest time, its coverage is more than TSC4.

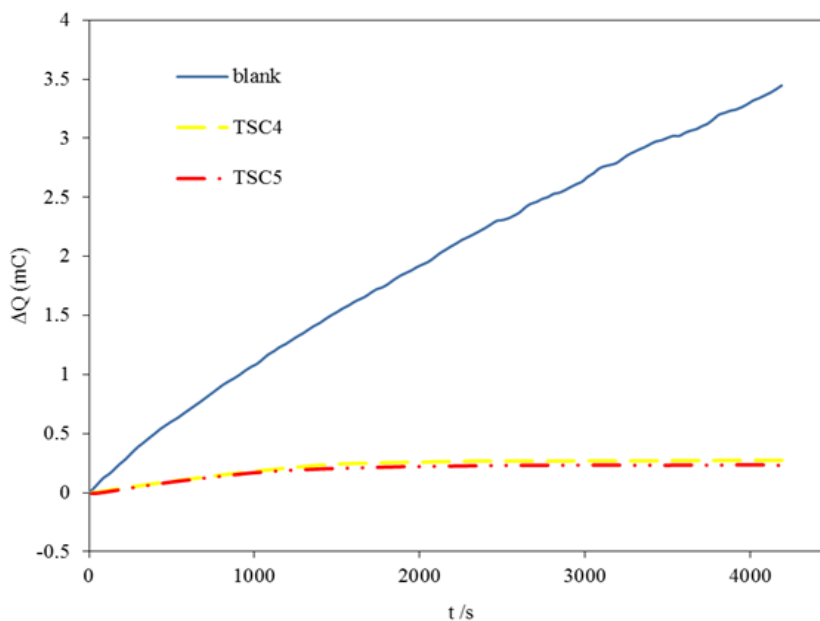


**Figure 7.** Plot of total charge ( $\Delta Q$ ) loaded by carbon steel electrode vs. time in the blank solution and the solution containing  $5.0 \times 10^{-4}$  M TSC4 and TSC5.

3.4. Surface analysis

Figure 8a, b, c and d represent the SEM images obtained for carbon steel samples before and after 24 h exposure to 1.0 M HCl in the absence and presence of  $1 \times 10^{-3}$  M TSC4 and TSC5.

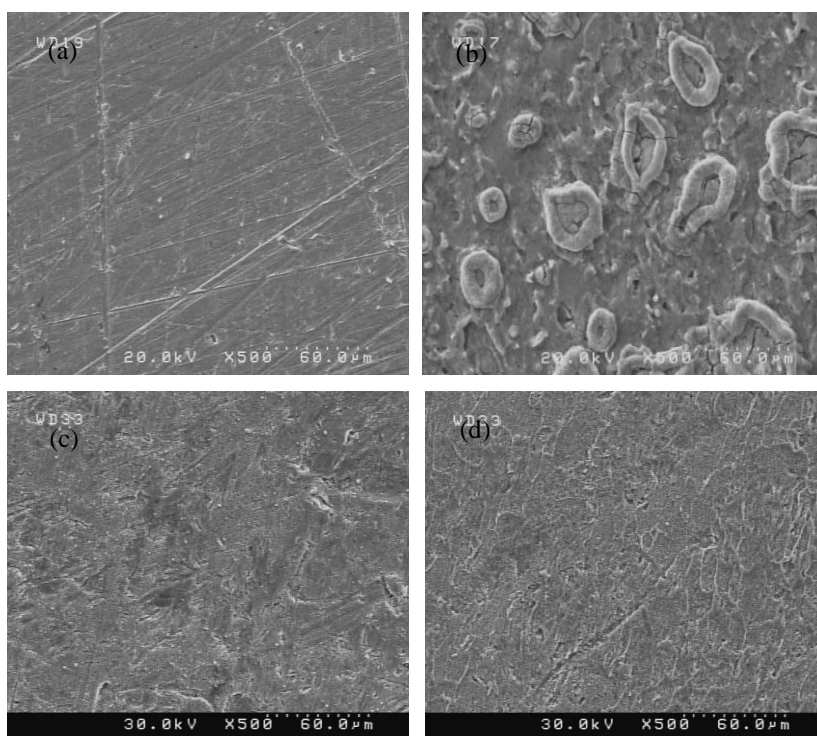


**Figure 8.** SEM micrographs of carbon steel samples for freshly polished surface (a) and after 24 h immersion in 1.0 M HCl without inhibitors (b) and with  $1.0 \times 10^{-3}$  M TSC4 (c) and TSC5 (d).

In Figure 8a, it can be seen that the carbon steel surface becomes fresh after abrading with emery papers showing some polishing scratches on the surface. Figure 8b shows the highly corroded surface due to the corrosive attack of HCl solution. A comparison between the images in the Figure 8b with those in 8c and d illustrates the diminish of the corrosion rate, which comes from the adsorption of the inhibitors on the carbon steel surface leading to reduction of the reaction sites on the surface. This results in an improvement in the surface characteristics of carbon steel immersed in the solutions containing TSC4 (Figure 8c) and TSC5 (Figure 8d).

### 3.5. Theoretical studies

In order to investigate the effect of geometrical and electronic features of the studied thiosemicarbazide compounds on their inhibition efficiencies, DFT calculations were done for the inhibitors TSC1-5 (Figure 1), which were studied either in this paper or in our previous works [35,36]. The optimized geometries, HOMO and LUMO distributions of five investigated molecules are presented in Figure. 9. At the figure, it could be seen that none of the inhibitor molecules are fully planar. However, the planarity is just one of the factors, which significantly makes good effect on the inhibitors efficiency. Also, the inhibitors performances depend on their electronic parameters. We should consider that the center of adsorption depends not only on the presence of HOMO and LUMO density on the special groups, which are oriented toward the steel surface, but also on the approachability of the interaction site, the partial charge and the local reactivity of the atom or group. The HOMO and LUMO density distributions of the studied molecules are shown in Figure 9. For the inhibitors TSC1, TSC2, and TSC3, the NH<sub>2</sub> group at one end of the molecule has minimum or no density of the FMO distributions. Other parts of the molecules have partial contributions from the HOMO and LUMO populations. For the inhibitors TSC4 and TSC5, HOMO is mainly focused on the thiocarbonyl group and LUMO is distributed on a part of the molecules, which contains benzamide group. Other side of both molecules, which ends to methoxybenzene for TSC4 and furan for TSC5, has no contributions of FMO densities.

In order to find a logical explanation for the relative inhibition effect of five thiosemicarbazides, we also need to consider the value of quantum chemical parameters in parallel with the spatial and electronic structure of the studied inhibitors. Table 3 shows the values of  $E_{\text{HOMO}}$ ,  $E_{\text{LUMO}}$ ,  $\Delta E$  and  $D$ , which are calculated with DFT method at B3LYP/6-31g(d,p) level of theory.

To better understand the relationship between quantum chemical parameters and the inhibition performances, the IE% values are correlated with the calculated parameters as quantum descriptors and shown in Figure 10a-d. According to the figure, the  $\Delta E$  has the highest correlation ( $R^2=0.97$ ) with IE% and  $E_{\text{LUMO}}$  has the second position ( $R^2=0.90$ ). The regression coefficient for dipole moment correlation is equal to 0.66 and  $E_{\text{HOMO}}$  shows no correlation with the IE%.

Figure 10a shows that  $\Delta E$  is correlated with IE% with a negative slope.  $\Delta E$  is an important parameter to estimate the reactivity of a molecule. A molecule with high energy gap is resistant toward the deformation or polarization of the electron cloud under small perturbation of chemical response. As

$\Delta E$  decreases, the reactivity of the molecule increases, leading to an increase in adsorption of inhibitor molecules on the metallic surface and consequently an increase in the IE% value [60,61].

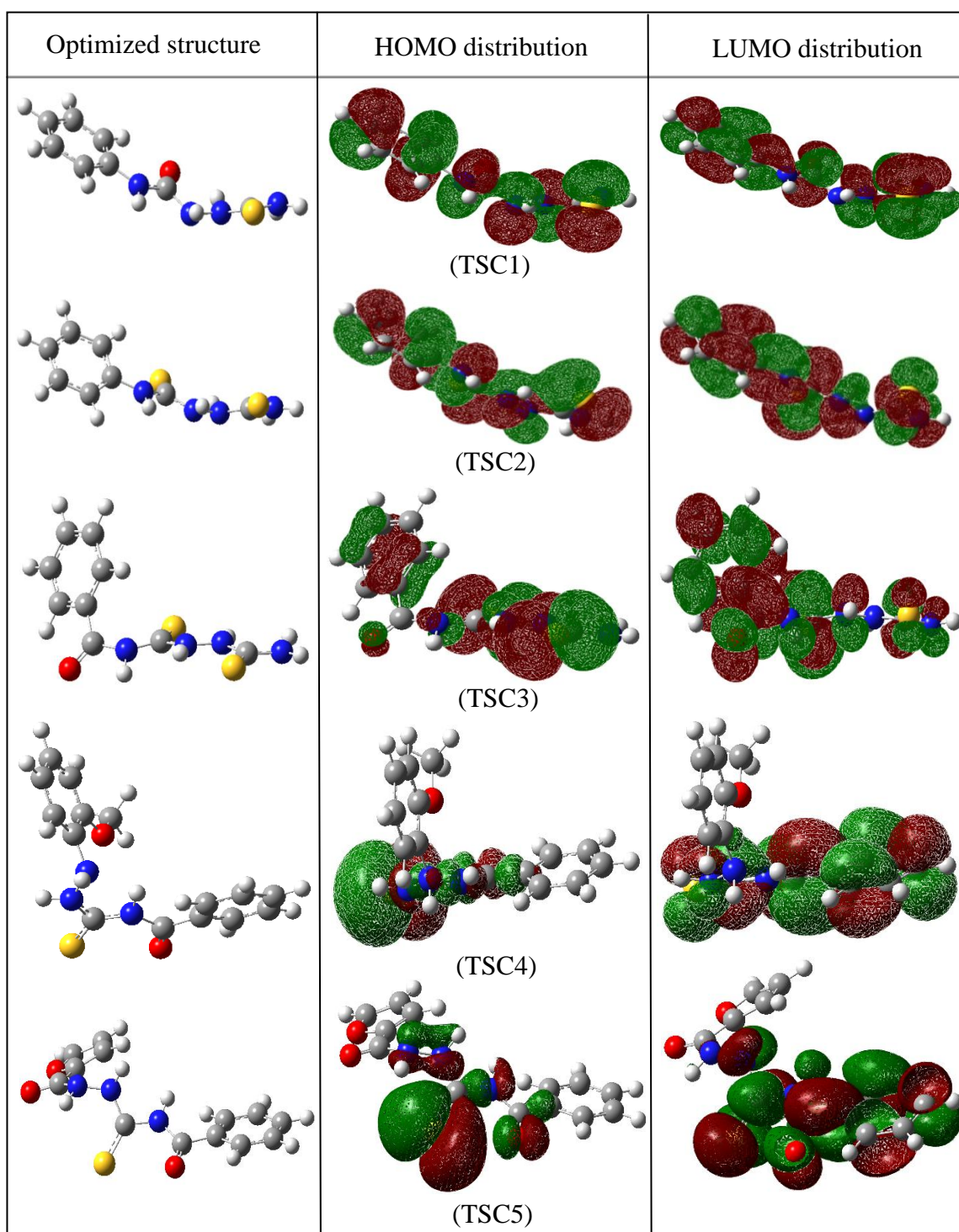
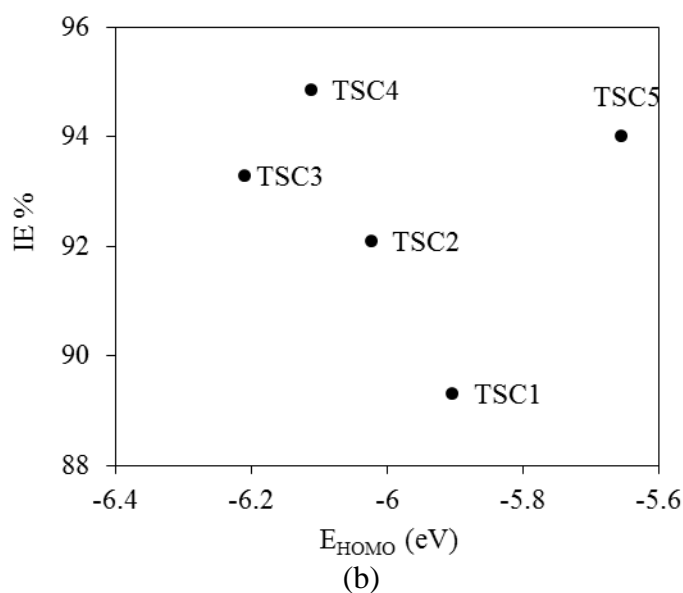
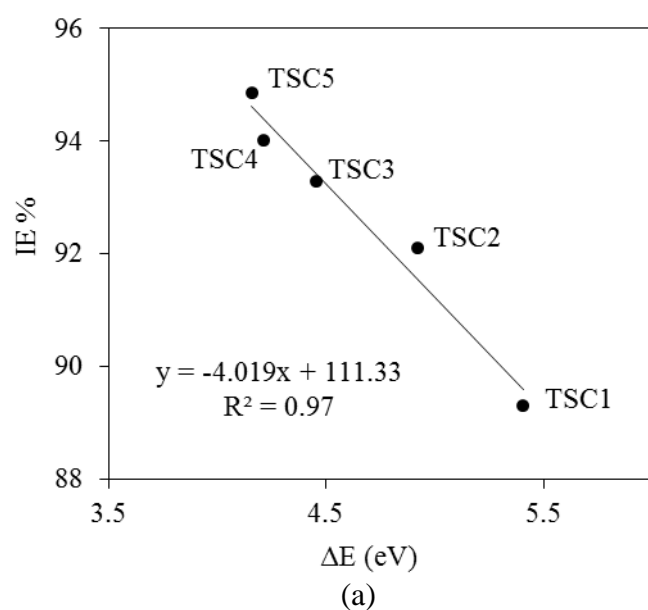


**Figure 9.** The optimized geometries and molecular orbital distributions of TSC1, TSC2, TSC3, TSC4 and TSC5, which are calculated at B3LYP/6-31G(d,p) level of DFT.

**Table 3.** Some quantum chemical parameters for the studied thiosemicarbazide inhibitors calculated using B3LYP/6-31G(d,p) level of DFT.

Inhibitor	$E_{\text{HOMO}}$ (eV)	$E_{\text{LUMO}}$ (eV)	$\Delta E$ (eV)	D (Debye)
TSC1	-5.90	-0.50	5.41	1.65
TSC2	-6.02	-1.01	4.92	1.03
TSC3	-6.21	-1.75	4.46	4.23
TSC4	-5.65	-1.44	4.21	5.37
TSC5	-6.11	-1.95	4.16	9.14

Figure 10b represents that  $E_{\text{HOMO}}$  is not well correlated to inhibition efficiencies. So in this system, the theoretical  $E_{\text{HOMO}}$  values cannot be used to predict the inhibition efficiencies of the inhibitors. It could be concluded that some other factors affect the experimental results.



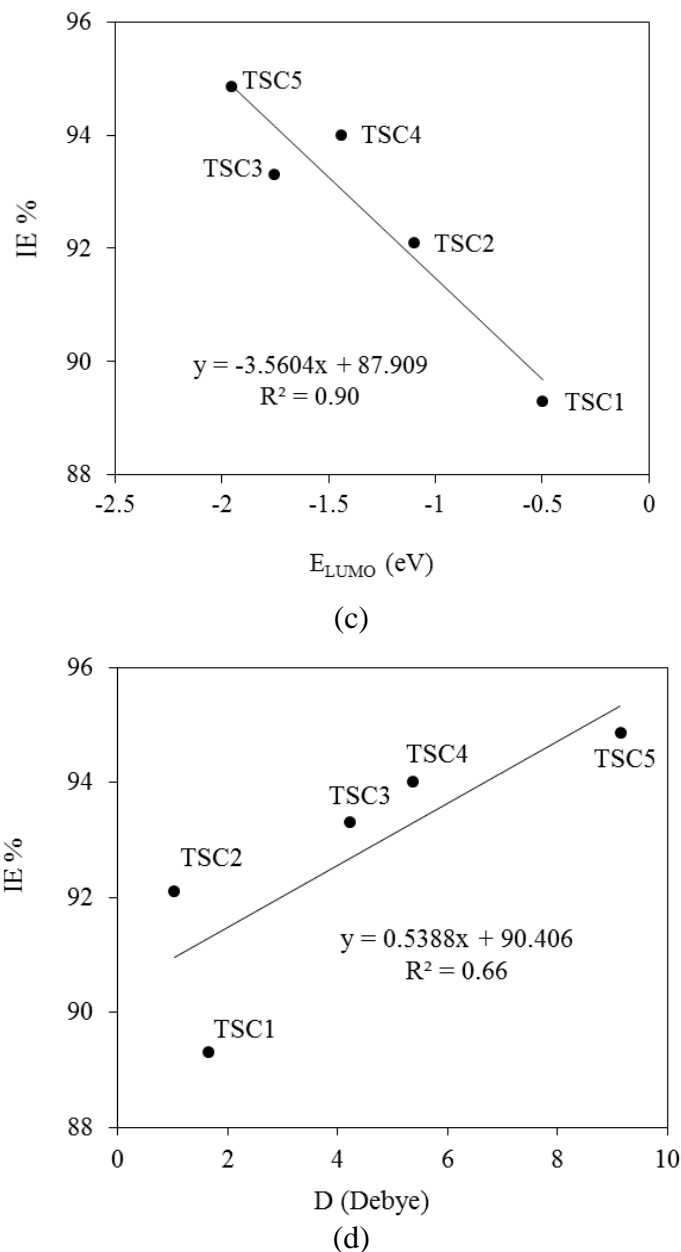


**Figure 10.** Variation of IE% with  $\Delta E$  (a),  $E_{\text{HOMO}}$  (b),  $E_{\text{LUMO}}$  (c) and the dipole moment (d) of TSC1, TSC2, TSC3, TSC4 and TSC5.

On the other hand,  $E_{\text{LUMO}}$  is related to the electron accepting ability of the molecule. In previous works, it was found that the inhibitors that can accept electrons from metallic surface along with donate electrons to the surface would be better inhibitors [62]. As shown in Figure 10c,  $E_{\text{LUMO}}$  is correlated to IE% with a negative slope. The decrease in  $E_{\text{LUMO}}$  values can lead to increase in inhibition effect of the inhibitors. So, the values of  $E_{\text{LUMO}}$  could well describe the experimental results. The next calculated quantum chemical parameter, dipole moment (D), is the measure of net molecular polarity. In some cases, the IE% values increases with increasing the value of the dipole moment. However, in most cases no significant relationship has been found between the dipole moment and the IE% [63-66]. Finally, there is not an agreement as a rule for the relation between the dipole moment and the inhibition efficiency. In this study, dipole moment is correlated to IE% with  $R^2=0.66$ . It could

be stated that higher values of dipole moment lead to an increase in the dipole-dipole interactions between the inhibitor and carbon steel surface. This enhancement results in better adsorption and higher inhibition effect.

#### 4. CONCLUSION

In the present study, the inhibition effect of two thiosemicarbazide derivatives on carbon steel corrosion in 1.0 M HCl was investigated by PDP, EIS, FFTCCV and SEM methods. PDP results showed that the studied compounds were mixed-type corrosion inhibitors with predominantly anodic inhibition effect. In the presence of the inhibitors, both anodic and cathodic Tafel slopes were changed and the corrosion current density decreased. The increase in the polarization resistance and decrease in the double layer capacitance with addition of the inhibitors are indications of their placement on the electrode surface leading to extension of the electrical double layer. Using FFTCCV, it could be possible to continuously monitor the current and charge, which passed through the electrode during immersion in 1.0 M HCl. It was found that for the studied thiosemicarbazide inhibitors, the rate of changes in current and charge was rationally high at the beginning of the experiment and gradually reached to nearly constant values at the end of each run. In addition, the results showed that for these inhibitors, the more effective one (TSC5) reached earlier to its maximum surface coverage. SEM observations also confirmed the improvement of the carbon steel surface physical appearance in the presence of the studied organic inhibitors.

In the other part, DFT calculations were done to optimize the molecular geometries of the studied inhibitors and calculate some electronic descriptors of the molecules. The obtained results were utilized in parallel with previous findings for three other thiosemicarbazide derivatives to give information about the inhibition mechanism of these compounds and the relationship between their inhibition efficiencies and electronic parameters. It was seen that the parameters  $\Delta E$  and  $E_{LUMO}$  showed the highest correlation coefficients respectively;  $D$  showed less correlation and  $E_{HOMO}$  presented no correlation with IE% values.

#### ACKNOWLEDGEMENTS

The authors express their appreciation to the University of Tehran Research Council for financial support of this work.

#### References

1. Davis & Associates, J. R. Davis (Ed.), Corrosion: understanding the basics, ASM International, (2000) Materials Park, Ohio, USA.
2. A. Groysman, Corrosion for everybody, Springer, (2010) Springer Science & Business Media B.V., Netherlands.
3. S. R. Rao, Resource recovery and recycling from metallurgical wastes, Elsevier (2006).
4. E. Garcia-Ochoa, S. J. Guzmán-Jiménez, J. Guadalupe Hernández, T. Pandiyan, J. M. Vásquez-Pérez and J. Cruz-Borbolla. *J. Mol. Struct.*, 1119 (2016) 314.

5. A. Zarrouk, H. Zarrokb, Y. Ramli, M. Bouachrine, B. Hammouti, A. Sahibed-dine and F. Bentiss, *J. Mol. Liq.*, 222 (2016) 239.
6. . K. O. Sulaiman and A. T. Onawole, *Comp. Theor. Chem.*, 1093 (2016) 73.
7. M. El Azzouzi, A. Aouniti, S. Tighadouin, H. Elmsellem, S. Radi, B. Hammouti, A. El Assyry, F. Bentiss and A. Zarrouk, *J. Mol. Liq.*, 221 (2016) 633.
8. M. Bouanis, M. Tourabi, A. Nyassi, A. Zarrouk, C. Jama and F. Bentiss, *Appl. Surf. Sci.*, 389 (2016) 952.
9. M. A. Hegazy, F. M. Atlam, *J. Mol. Liq.*, 218 (2016) 649.
10. N. Yilmaz, A. Fitoz, Ü. Ergun and K. C. Emregül, *Corros. Sci.*, 111 (2016) 110.
11. A. Varvaressou, A. Tsantili-Kakoulidou, T. Siatra-Papastaikoudi and E. Tiligada, *Arzneim. Forsch.*, 50 (2000) 48.
12. A. M. Omar, A. M. Farghaly, A. A. Hazzai, N. H. Eshba, F. M. Sharabi and T. T. Daabees, *Pharm. Sci.*, 70 (1981) 1075.
13. M. Sai, Sh. Zhong, Y. Tang, W. Ma, Y. Sun and D. Ding, *J. App. Polym. Sci.*, 131 (2014) 40535.
14. J. N. Reshma and S. Avinash, *Der. Pharma. Chemica*, 5 (2013) 45.
15. M. K. Biyala, N. Fahmi and R.V. Singh, *Indian J. Chem.*, 45A (2006) 1999.
16. T. Plech, M. Wujec, A. Siwek, U. Kosikowska and A. Malm, *Eur. J. Med. Chem.*, 46 (2011) 241.
17. A. Siwek, P. Stańczek and J. Stefańska, *Eur. J. of Med. Chem.*, 46 (2011) 5717.
18. I. R. Ezabadi, C. Camoutsis, P. Zoumpoulakis, A. Geronikaki, M. Soković, J. Glamočilija and A. Ćirić, *Bioorg. Med. Chem.*, 16 (2008) 1150.
19. S. Zor, H. Özkazanç, T. Arslan and F. Kandemirli, *Corrosion*, 66 (2010) 045006.
20. S. M. Abd El Haleem, S. Abd El Wanees, E.E. Abd El Aal and A. Farouk, *Corros. Sci.*, 68 (2013) 1.
21. P. Mohan and G. Paruthimal Kalaigna, *J. Mater. Sci. Technol.*, 29 (2013) 1096.
22. A. Y. Musa, A. A. H. Kadhum, A. B. Mohamad and M. S. Takriff, *Mater. Chem. Phys.*, 129 (2011) 660.
23. G. E. Badr, *Corros. Sci.*, 51 (2009) 2529.
24. A. A. Gürten, K. Kayakırlmaz and M. Erbil, *Constr. Build. Mater.*, 21 (2007) 669.
25. A. B. Tadros and M. El-Batouti, Anti-Corros., *Methods Mater.*, 51 (2004) 406.
26. I. J. Casely, J. W. Ziller, M. Fang, F. Furche and W. J. Evans, *J. Am. Chem. Soc.*, 133 (2011) 5244.
27. N. O. Obi-Egbedi and I. B. Obot, *Arab. J. Chem.*, 6 (2013) 211.
28. I. Danaee, O. Ghasemi, G. R. Rashed, M. Rashvanavei and M. H. Maddahy, *J. Mol. Struct.*, 1035 (2013) 247.
29. A. H. El-Askalany, S. I. Mostafa, K. Shalabi, A. M. Eida and S. Shaaban, *J. Mol. Liq.*, 223 (2016) 497.
30. A. K. Singh, S. Khan, A. Singh, S. M. Quraishi, M. A. Quraishi and E. E. Ebenso, *Res. Chem. Intermed.*, 39 (2013) 1191.
31. A. Zarrouk, I. El Ouali, M. Bouachrine, B. Hammouti, Y. Ramli, E.M. Essassi, I. Warad, A. Aouniti and R. Salghi, *Res. Chem. Intermed.*, 39 (2013) 1125.
32. N. A. Wazzan, I.B. Obot and S. Kaya, *J. Mol. Liq.*, 222 (2016) 239.
33. S. John, K. M. Ali and A. Joseph, *Bull. Mater. Sci.*, 34 (2011) 1245.
34. M. A. Bedair, *J. Mol. Liq.*, 219 (2016) 128.
35. S. Shahabi, P. Norouzi and M. R. Ganjali, *Anal., Bioanal., Electrochem.*, 6 (2014) 260.
36. S. Shahabi, P. Norouzi and M. R. Ganjali, *RSC Adv.*, 5 (2015) 20838.
37. M. J. Frisch, G. W. Trucks, H. B. Schlegel, G. E. Scuseria, M. A. Robb, et al., Gaussian Inc., (2004) Wallingford CT.
38. Standard practice for conventions applicable to electrochemical measurements in corrosion testing. ASTM G3-89, (1994).
39. J. O. L. Riggs and C.C. Nathan (Ed.), Corrosion inhibitors, 2nd ed., NACE, (1973) Houston, TX, USA.

40. J. Saranya, M. Sowmiya, P. Sounthari, K. Parameswari, S. Chitra and K. Senthilkumar, *J. Mol. Liq.*, 216 (2016) 42.
41. E. S. Ferreira, C. Giancomelli, F. C. Giacomelli and A. Spinelli, *Mater. Chem. Phys.*, 83 (2004) 129.
42. D. K. Singh, S. Kumar, G. Udayabhanu and R. P. John. *J. Mol. Liq.*, 216 (2016) 738.
43. I. Ahamad, C. Gupta, R. Prasad and M. A. Quraishi, *J. Appl. Electrochem.*, 40 (2010) 2171.
44. M. Yadav, L. Gope, N. Kumari and P. Yadav, *J. Mol. Liq.*, 216 (2016) 78.
45. M. Behpour, S. M. Ghoreishi, N. Mohammadi, N. Soltani and M. Salavati-Niasari, *Corros. Sci.*, 52 (2010) 4046.
46. F. B. Growcock and J. H. Jasinski, *J. Electrochem. Soc.*, 136 (1989) 2310.
47. R. Mohan, K. Ramya, K. K. Anupama and A. Joseph, *J. Mol. Liq.*, 220 (2016) 707.
48. J. E. Randles, *Discuss. Faraday Soc.*, 1 (1947) 11.
49. C. S. Hsu and F. Mansfeld, *Corrosion*, 57 (2001) 747.
50. X. Li, S. Deng, H. Fu and G. Mu, *Corros. Sci.*, 51 (2009) 620.
51. K. Babic-Samardzija, C. Lupu, N. Hackerman, A. R. Barron and A. Lutge, *Langmuir*, 21 (2005) 12187.
52. F. Bentiss, C. Jama, B. Mernari, H. El Attari, L. El Kadi, M. Lebrini, M. Traisnel and M. Lagrenee, *Corros. Sci.*, 51 (2009) 1628.
53. P. Norouzi, M. Pirali-Hamedani, T. M. Garakani, M. R. Ganjali and G. Nikolic (Ed.). Application of Fast Fourier Transforms in some advanced electroanalytical methods; Fourier Transforms, new analytical approaches and FTIR strategies, InTech, (2011) Croatia.
54. M. R. Ganjali, P. Norouzi, R. Dinarvand, R. Farrokhi and A. A. Moosavi-Movahedi, *Mater. Sci. Eng. C*, 28 (2008) 1311.
55. S. Shahabi, P. Norouzi and M. R. Ganjali, *Int. J. Electrochem. Sci.*, 10 (2015) 2646.
56. S. Shahabi, P. Norouzi and M. R. Ganjali, *Russian J. Electrochem.*, 51 (2015) 833.
57. P. Norouzi, B. Larijani, M. R. Ganjali and F. Faridbod, *Int. J. Electrochem. Sci.*, 7 (2012) 10414.
58. P. Norouzi, H. Rashedi, T. M. Garakani, R. Mirshafian and M. R. Ganjali. *Int. J. Electrochem. Sci.*, 5 (2010) 377.
59. P. Norouzi, V. K. Gupta, F. Faridbod, M. Pirali-Hamedani, B. Larijani and M. R. Ganjali, *Anal. Chem.*, 83 (2011) 1564.
60. Z. El Adnani, M. Mcharfi, M. Sfaira, M. Benzakour and A. T. Benjelloun, *Corros. Sci.*, 68 (2013) 223.
61. N. Soltani, N. Tavakkoli, M. Khayatkashani, M. R. Jalali and A. Mosavizade, *Corros. Sci.*, 62 (2012) 122.
62. G. Trabenelli and F. Mansfeld (Eds.), *Corrosion mechanisms*, Marcel Dekker, (1987) USA.
63. X. Li, S. Deng, H. Fu and T. Li, *Electrochim. Acta*, 54 (2009) 4089.
64. N. Khalil, *Electrochim. Acta*, 48 (2003) 2635.
65. L. Rodriguez-Valdez, A. Martinez-Villafañe and D. Mitnik, *J. Mol. Struct.*, 713 (2005) 65.
66. G. Gao and C. Liang, *Electrochim. Acta*, 52 (2007) 4554.